Power-law scaling in human EEG: Relation to Fourier power spectrum

*Thomas C. Ferree[1] and Rudolph C. Hwa[2]

[1] *Dynamic Neuroimaging Laboratory, Department of Radiology, University of California San Francisco*

[2] *Institute of Theoretical Science and Department of Physics, University of Oregon*

October 18, 2002

Abstract

We discuss a method of analyzing spontaneous human EEG time series, which emphasizes scale-independent behavior. We use detrended fluctuation analysis to quantify the temporal fluctuations as a function of window width, and show how power-law scaling behavior is frequently manifest over two distinct temporal ranges. These ranges encompass time scales associated with meaningful aspects of cortical physiology. This paper shows a simple way of quantifying the existence of such scaling behavior, and determining the characteristic time scale which separates the two regions. By making a qualitative connection with the discrete Fourier transform, we show how the violation of scaling between the two regions is associated with the normal human alpha rhythm, but that the existence scale-independent behavior on either side of the alpha rhythm enables a succinct description of the complex dynamics not accessible in the Fourier power spectrum.

Keywords: Electroencephalography, fractal, complexity, alpha rhythm.

In Press: *Neurocomputing (2003)*

1 Introduction

The human brain is obviously a complex system, and exhibits rich spatiotemporal dynamics. Among the noninvasive techniques for probing human brain dynamics, scalp electroencephalography (EEG) provides a direct measure of cortical activity with millisecond temporal resolution [10]. Because the spatial resolution at the scalp is low, EEG time series reflect the integrated activity of large neural populations. But such large-scale integration is not necessarily a shortcoming of EEG, because it is well established that neural activity at this scale is correlated with brain function and disease. Thus a practical goal is to effectively characterize the complex EEG waveforms with a minimum of assumptions, then study inferences from these dynamical measures.

We restrict our attention to the ongoing spontaneous EEG, rather than the event-related response functions. The most commonly used technique for analyzing spontaneous EEG is the Fourier power spectrum, based upon decomposing the signal into a linear sum of sinusoidal waves each with constant phase [13]. Clearly this has limitations for describing nonlinear and nonstationary systems. Recognizing the nonlinear aspect, chaos theory has also been applied [3]. While in certain cases the EEG does appear to exhibit low-dimensional chaotic dynamics, e.g., epileptic seizure [1], EEG dynamics are generally so high-dimensional that establishing the existence of stable attractors

*Corresponding author. Telephone: (415) 502-3726; Email: tom.ferree@radiology.ucsf.edu

is challenged by system nonstationarity, i.e., slowly changing variables or parameters which may change attractor properties [11, 4].

We describe here an alternative approach, which avoids the assumptions of linearity and low-dimensional attractors, and emphasizes instead scale-independent behavior in a certain measure of the temporal fluctuations. Power-law scaling behavior is definitive of fractals, but is also nearly ubiquitous in complex systems, arising in a variety of different quantifications of the data [5]. From the viewpoint of theoretical physics, this fact is of great interest, because scaling phenomena are known to occur in thermodynamic systems near a criticial state, with interesting implications for how perturbations may propagate through the system [2]. We make no claim here that our analysis shows the brain is in a critical state, although this theoretical backdrop did inspire our initial inquiry. Instead we emphasize here the practical determination of scaling behavior in real data, and make qualititative comparisons with the Fourier power spectrum. Other papers demonstrate the successful application of scaling analysis to the clinical problem of acute stroke detection [6, 7].

2 Scaling analysis of EEG time series

The fluctuations F in a system, computed as a function of some scale k, are said to be scale-independent if

$$F(k) \propto k^{\alpha} \ . \tag{1}$$

because the dependence on k is invariant under a scale transformation $k \to ck$. If (1) holds, then the exponent α provides a succinct measure of the dynamics across a range of k. Equation (1) implies $\ln F \propto \alpha \ln k$, thus linear regions in plots of $\ln F$ versus $\ln k$ indicate power-law behavior, with the slope of the line given by the exponent α. For ideal mathematical fractals, such behavior persists without limit in k. For physical systems, its range is always finite, and may in addition be interrupted by dynamical mechanisms which introduce characteristic time scales into the data.

To quantify the fluctuations in an EEG time series, we use a variant of detrended fluctutation analysis (DFA) [12], adapted to continuous time series [6, 7]. The detrending renders the method relatively insensitive to nonstationarities in the data. To define $F(k)$, let an EEG time series be denoted by $V(t)$, where t is discrete time ranging from 1 to T. Divide the entire range of t to be investigated into B equal windows, discarding any remainder, so that each window has $k = \text{floor}(T/B)$ time points. Within each window, labeled b ($b = 1, \ldots, B$), perform a least-square fit of $V(t)$ by a straight line, $\overline{V}_b(t)$, i.e., $\overline{V}_b(t) = \text{Linear-fit}[V(t)]$ for $(b-1)k < t \leq bk$. That is the semi-local trend for the bth window. The squared fluctuation from the semi-local trend in the bth window is defined

$$F_b^2(k) = \frac{1}{k} \sum_{t=1+(b-1)k}^{k+(b-1)k} [\, V(t) - \overline{V}_b(t)\,]^2 \ . \tag{2}$$

This quantity is averaged over B windows to yield

$$F(k) = \sqrt{\frac{1}{B} \sum_{b=1}^{B} F_b^2(k)} \ . \tag{3}$$

The algorithm gives a measure of the fluctuations on scale k with a minimum of assumptions about the nature of the signal. The measure $F(k)$ has a useful theoretical limit: an uncorrelated random walk gives $\alpha = 1/2$ analytically, and other values of α reveal temporal correlations [9].

Figure 1a shows the first 0.5 sec of three 10-second EEG times series for a normal subject, resting with eyes closed. The data were hardware filtered between 0.1 Hz and 100 Hz, and digitized at 250 Hz. The semi-local trends $\overline{V}_b(t)$ are shown as dashed lines. Figure 1b shows plots of $\ln F$ versus $\ln k$ for the three channels in Fig. 1a, for values of k from 5 to 250, in approximately equal steps of $\ln k$. For each channel shown, it is evident that power-law behavior exists over two temporal regions. We call the slopes of the two lines α_1 and α_2, corresponding to short and long time scales, respectively. We have analyzed 128 EEG time series for a total of 28 normal subjects [7], and found similar behavior in nearly all cases. There are certainly exceptions to the rule, the most common being that it may be necessary to allow for a transitional region in which the bend is not so sharp. Still this is strikingly simple behavior for such complex data sets. Even the rare violations of scaling might themselves prove informative.

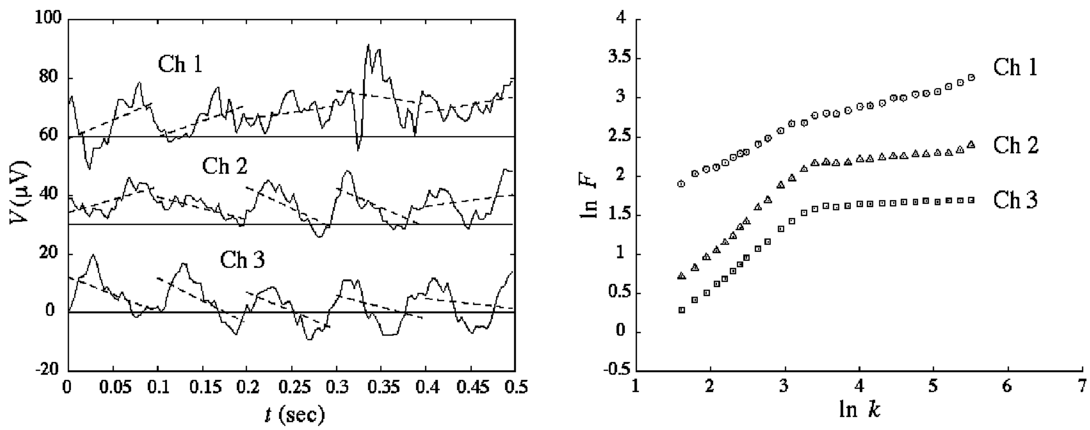

Figure 1: (a) Examples of EEG time series in three channels for a single subject. The vertical scales of Ch. 1 and Ch. 2 are shifted upward by 60 and 30 μV, respectively. Dashed lines indicate semi-local trends for $k\Delta t = 0.1$ s. (b) $\ln F$ versus $\ln k$ for the three channels in (a). The vertical scales of Ch. 1 and Ch. 2 are shifted upward by 1.0 and 0.5 units, respectively. Errors in $\ln F$ are shown with vertical lines (mostly appearing as dots) inside plot symbols (see Section 3).

3 Fitting scaling exponents

To determine the values of α_1 and α_2, we must decide how to fit lines to the curves in Fig. 1b. One way is to define two regions which are well separated from the bend so as to provide reasonable fits for all available data. This was the approach taken in [6, 7] where it was found that $1 < \ln k < 2.5$ (Region 1) and $3.5 < \ln k < 5.75$ (Region 2) do a reasonable job for all 28 subjects studied so far. It is obviously of interest to automate this process, to obtain more objective channel-specific definitions of the two regions. When the bend is sharp as in Fig. 1b, this may be done simply by allowing a single match point between two contiguous regions to be a free parameter, which is varied to minimize the overall fitting error.

Optimally fitting lines to the curves in Fig. 1b requires estimates of the errors in $\ln F$. There are three main sources of error in the original voltage data $V(t)$. First, the EEG amplifiers introduce to each time point a Gaussian random variable with RMS amplitude 0.6 μV. Second, there is often a slow drift associated with changing quality of scalp-electrode contact, but fortuitously this tends to be removed by the detrending in DFA. Third, approximation of potentials relative to infinity via the average reference [10], used here, or any technique for deconvolving scalp potentials to the brain surface, introduces further errors in the signal to be analyzed. To illustrate the procedure here, we consider only errors due to amplifier noise. In accordance with data, we assume amplifier noise is stationary and normally distributed, with RMS amplitude denoted by $\delta V = 0.6$ μV.

In each window b, the local linear trend $\overline{V}_b(t) = a_b + m_b t$ is obtained using standard linear regression. Along with the maximum likelihood parameters of the line (a_b, m_b), errors in the estimates of these parameters $(\delta a_b, \delta m_b)$ may also be obtained. It is straightforward to account for each of these contributions when computing $F(k)$. We first define an array containing the complete list of quantities on which F depends: $\{r_j\} = \{V_b(t), \{a_b\}, \{m_b\}\}$, where $j = 1, \ldots, kB + 2B$, and consider $F = F(k; \{r_j\})$. Assuming each r_j has a Gaussian random error δr_j, and makes an independent contribution to $F(k;\{r_j\})$, these contributions combine in quadrature according to

$$\delta F(k) = \left[\sum_{j=1}^{(k+2)B} \left(\frac{\partial F}{\partial r_j} \right)^2 \delta r_j^2 \right]^{1/2} . \tag{4}$$

Taking the derivates $\partial F/\partial r_j$ leads to

$$\delta F(k) = \left[\frac{1}{kB} \delta V^2 + \frac{1}{F^2} \frac{1}{B^2} \sum_{b=1}^{B} \left(\left\langle V - \overline{V} \right\rangle_b^2 \delta a_b^2 + \left\langle (V - \overline{V}) \tau \right\rangle_b^2 \delta m_b^2 \right) \right]^{1/2} \tag{5}$$

where $<>_b$ denotes an average over the bth window, and $\tau = (1, \ldots, k)$ is a vector containing the discrete time points in the local coordinates of window b. We allowed the trend errors δa_b^2 and δm_b^2 to depend upon b, since that was found numerically to be the case. To compute the errors in $\ln F$, we trivially compute

$$\delta \ln F(k) = \frac{1}{F(k)} \, \delta F(k) \tag{6}$$

which has the effect of increasing the error $\delta \ln F$ at small values of F, i.e., small values of k. This gives the error bars shown in Figure 1b.

To fit the linear behavior in Fig. 1b, we assume there exist two linear regions, which meet at a single point $\ln k = \ln \kappa$. For each value of $\ln \kappa$, we use standard linear regression to compute best-fit lines for the two regions. In each region the best fit line is defined as the one which minimizes χ^2, and the best overall fit is determined by the minimum of the total error $E = \chi_1^2 + \chi_2^2$. Fig. 2a shows the error E as a function of $\ln \kappa$, with a clear minimum for each channel. Figure 2b shows the optimal fits for each channel, the slopes of the lines giving the scaling exponents α_1 and α_2. When this procedure works, the value of κ reveals a characteristic time scale in the data, and the minimum error $E_{\min}$ gives a measure of the overall quality of the scaling behavior.

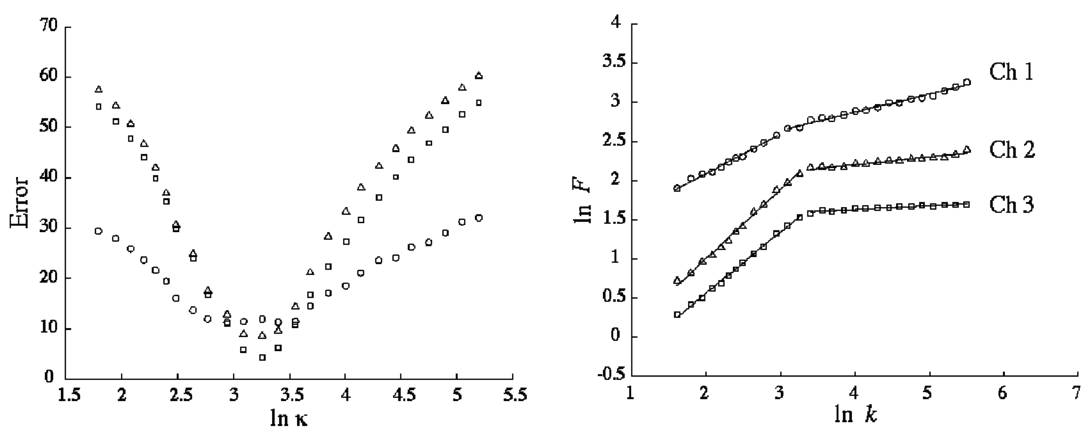

Figure 2: (a) Fit error E versus bend location $\ln \kappa$ for Chs. 1-3. (b) Optimal linear fits for Chs. 1-3, with slopes equaling α_1 and α_2. Plot symbols are the same as in Fig. 1b.

4 Relation to Fourier power spectrum

The most common method of analyzing spontaneous EEG time series is the Fourier transform. Because of how this analysis tool relates to linear systems, the emphasis is usually placed on individual peaks in the power spectrum, which are implicitly interpreted as resonant frequencies. In contrast, scaling analysis considers the entire continuum of time scales when present, and emphasizes the often simple relationships *across* time scales [2, 5]. Within Fourier analysis a close analogy is asking whether the power spectrum behaves as $P(f) \propto 1/f^{\beta}$. This is a form of scaling analysis, but still relies upon decomposing the signal into a linear superposition of sinusoidal waves.

We computed the Fourier power spectrum for the three time series in Fig. 1a. Each 10-second data segment was divided into ten 1-second segments. Each 1-second segment was Hann windowed, then Fourier transformed using a standard FFT algorithm. This gives 1 Hz frequency resolution. The Fourier amplitude $A(f) \equiv \sqrt{P(f)}$ was computed by taking the complex modulus and averaging over the ten 1-second segments. Figure 3a shows A versus f on linear-linear axes. A clear peak is evident near 10 Hz. Figure 3b shows A versus f on log-log axes. The peak near 10 Hz is still evident. At frequencies below the peak, $\ln A$ falls with $\ln f$, although not monotonically. At frequencies above the peak, the behavior is completely erratic. Clearly the DFA behavior in Fig. 1b is much more amenable to description with a few parameters, especially at shorter time scales and higher frequencies.

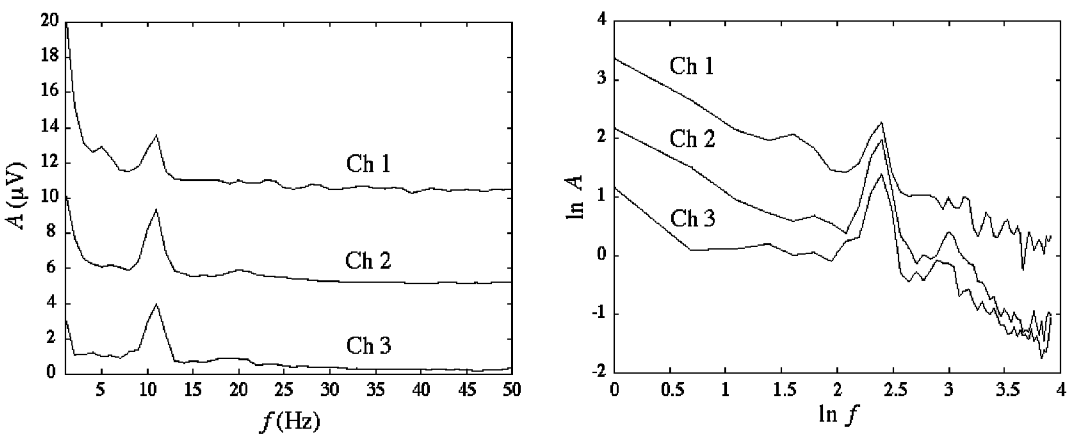

Figure 3: Power spectrum amplitude of the three time series in Fig. 1a. (a) Linear axes: The vertical scales of Ch. 1 and Ch. 2 are shifted upward by 10 and 5 μV, respectively. (b) Log-Log axes: The vertical scales of Ch. 1 and Ch. 2 are shifted upward by 1 and 0.5 units, respectively.

We have compared the results of DFA and Fourier analyses for the 28 subjects in Ref. [7]. The following observations are made: (1) The general tendency for $\ln F$ to increase with $\ln k$ is associated with the tendency for $\ln A$ to decrease with $\ln f$, because of the inverse relationship between time and frequency on the horizontal axis; (2) The characteristic time scale $\kappa\Delta t$ is associated with the dominant frequency $\ln f_{\max}$, which in these examples clearly represents the normal human alpha rhythm; (3) The behavior on either side of the characteristic time scale or frequency is always much smoother for $\ln F$ than $\ln A$, especially at shorter time scales (higher frequencies). This makes the results of the DFA approach more amenable to concise summary with a small number of parameters. Concise description is a stated objective when considering 128 channels across many subjects.

5 Discussion

We have described how a variant of detrended fluctuation analysis [6, 7] can be used to reveal scale-independent behaviors in spontaneous EEG time series. Although any possible relation to self-organized criticality [2] is not yet established, the scaling exponents provide a concise summary of the complex dynamics across physiologically meaningful time scales.

For most subjects and channels, strikely good power-law behavior is seen over two temporal regions, spanning an interesting breadth of physiological time scales. The two regions are separated by a characteristic time scale, which appears associated with the normal human alpha rhythm. This paper describes an objective way to define the two regions, and obtain channel-specific estimates of the characteristic time scale and overall quality of scaling behavior.

Acknowledgements

We thank Dr. Phan Luu and Prof. Don Tucker for supplying the EEG data for our analysis. This work was supported, in part, by the National Institutes of Health under Grant Nos. NS-38829 and NS-27900, and by the U.S. Department of Energy under Grant No. DE-FG03-96ER40972.

References

[1] Babloyantz, A. and A. Destexhe (1986). Low dimensional chaos in an instance of epilepsy. Proceedings of the National Academy of Sciences USA 83: 3513-3517.

[2] Bak, P. *How Nature Works: The Science of Self-Organized Criticality.* (Copernicus, 1996).

[3] *Chaos in Brain?* K. Lehnertz, J. Arnhold, P. Grassberger and C. E. Elger (Eds.) (World Scientific, 2000).

[4] Freeman, W. J. (2000). A proposed name for aperiodic brain activity: Stochastic chaos. Neural Networks 13: 11-13.

[5] Gisiger, T. (2001). Scale invariance in biology: Coincidence or footprint of a universal mechanism? Biol. Rev. 76: 161-209.

[6] Hwa, R. C. and T. C. Ferree (2002). Fluctuation analysis of human electroencephalogram. Nonlinear Phenomena in Complex Systems 5(3): 302-308.

[7] Hwa, R. C. and T. C. Ferree (2002). Scaling properties of fluctuations in human electroencephalogram. Physical Review E 66: 021901.

[8] Linkenkaer-Hansen, K., V. V. Nikouline, J. M. Palva and R. J. Ilmoniemi (2001). Long-range temporal correlations and scaling behavior in human brain oscillations. Journal of Neuroscience 21(4): 1370-1377.

[9] Montroll, E. W. and M. F. Schlesinger. In: *Nonequilibrium Phemonema II: From Stochastics to Hydrodynamics.* J. L. Lebowitz and E. W. Montroll, Eds. (North-Holland, 1984).

[10] Nunez, P. L. *Electric Fields of the Brain.* (Oxford University Press, 1981).

[11] Palus, M. (1996). Nonlinearity in normal human EEG: cycles, temporal asymmetry, nonstationarity and randomness, not chaos. Biological Cybernetics 75: 389-396.

[12] Peng, C.-K., J. Mietus, J. M Hausdorff, S. Havlin, H. E. Stanley, and . L. Goldberger (1993). Long-range anticorrelation and non-Gaussian behavior of the heartbeat. Physical Review Letters 70(9): 1343-1346.

[13] Walter, D. O. (1963). Spectral analysis for electroencephalograms: Mathematical determination of neurophysiological relationships from records of limited duration. Exp. Neurol. 8: 155-181.